Project Title:	Baltic+ SeaLaBio
Document Title:	Validation Report (VR) V2
Version:	2.3 Final version
Author(s) and affiliation(s):	Sampsa Koponen, Jenni Attila, Kari Kallio, Sakari Väkevä, SYKE Constant Mazeran, SOLVO Dagmar Müller, Carsten Brockmann, Carole Lebreton, BC Petra Philipson, BG Thomas Neumann, IOW
Version history:	2.0 Jan 24, 2020. Version for ESA review 2.1 Jun 25, 2020. Version for ESA review 2.2 Sep 30, 2020. Version for ESA review 2.3 Nov 20, 2020. Final version
Distribution:	Public

Contents

Abstract

This document describes the validation results of WP3 of the SeaLaBio project obtained until Sep 30, 2020.

Glossary

AC	Atmospheric correction
C2RCC	Care 2 Regional Coast Color
CDOM	Coloured Dissolved Organic Matter
aCDOM	Absorption coefficient of Coloured Dissolved Organic Matter
Chl a	Chlorophyll a
CMEMS	Copernicus Marine Environment Monitoring Service
DOC	Dissolved Organic Carbon
DOM	Dissolved Organic Matter
EO	Earth Observation
ERGOM	Ecological Regional Ocean Model
FT	Flow-Through
FUB	Free University of Berlin (EO processor)
HELCOM	Helsinki Commission
ICES	International Council for the Exploration of the Sea
IPF	Instrument Processing Facility (standard processor)
MERIS	Medium Resolution Imaging Spectrometer
MPD	Median Percentage Difference
MS	Monitoring station
MSI	Multi Spectral Instrument
NIR	Near infrared
NN	Neural Network
OC	Ocean Colour
OLCI	Ocean and Land Color Imager
POLYMER	POLYnomial based algorithm applied to MERIS
RMSE	Root Mean Square Error
RRMSE	Relative Root Mean Square Error
S2	Sentinel-2
S3	Sentinel-3
SAG	Scientific Advisory Group
TOA	Top of Atmosphere
TSM	Total Suspended Matter
WS	Water Sample

List of Symbols

Symbol	Definition	Dimension/Unit
ρ_a	Aerosol signal	dimensionless
ρ_{Rc}	Rayleigh corrected signal	dimensionless
ρ_w	Marine reflectance	dimensionless
$\rho_{wN}(\lambda)$	Marine reflectance, normalized	dimensionless
n	Number of data points	
M	Reference data	
O	Observed data	
r	Correlation	
R^2	Coefficient of determination	

1 Introduction

1.1 Scope

This document is the second version of the Validation Report of the SeaLaBio project. It includes the EO validation results obtained until Aug 31, 2020.

The validation for the ecosystem model ERGOM will be given in the Impact Assessment Report.

1.2 Basics of validation

In Earth Observation validation means the comparison of the values derived from EO data with the in situ values (i.e. the ground truth). Its main purpose is to find out how well the EO represents the reality and typically includes a variety of plots and statistics.

At the core of validation are matchups which consist of EO and in situ data pairs that have been observed from the same place during the same time. In practice, the "same time" requirement is difficult to achieve, and some amount of time difference has to be accepted. According to Matchup Protocols by EUMETSAT (2019) the time difference between an in situ measurement and a satellite overpass should be no longer than 1 hour. The protocol also stated that the time difference can be extended to 3 hours at the beginning of the mission to get more data points. Smaller differences are of course preferred, but in locations where temporal changes can be assumed to be small a larger time difference can be accepted. This choice must be made on case-by-case basis.

Also the "same place" requirement can be difficult to achieve. The water samples are taken from one location while the EO pixel represents a square with a size from 10 m to 300 m in our case. In locations with large horizontal gradients the variability of water parameters within one pixel can be substantial. Furthermore, some measurement platforms (boats and ships) can drift during the measurement, which creates further uncertainty.

Finally, if the bottom is visible the water quality parameters usually cannot be estimated. Thus, information about the depth of the station is important.

The typical statistics used in validation are shown in Table 1.

Table 1. Statistics typically used in validation of EO data.

Correlation (r)	$r(A,B) = \frac{1}{n-1}\sum_{i=1}^{n}\left(\frac{A_i-\mu_A}{\sigma_A}\right)\left(\frac{B_i-\mu_B}{\sigma_B}\right)$ where μ and σ are the mean and standard deviations.
Coefficient of determination (R^2)	$R^2 = r^2$
Root Mean Square Error (RMSE)	$RMSE = \sqrt{\frac{\sum(O-M)^2}{n}}$, where O is the observed data (satellite), M is the reference data (in situ) and n is the number of data points.
Relative Root Mean Square Error (RRMSE)	RRMSE = RMSE/mean(M) *100%
Bias	$Bias = \frac{1}{n}\sum(O-M)$
N	Number of matchup data points
Median Percentage Difference (MPD)	MPD = median(|O-M|/M)
Slope	The slope of the regression trend line
Intercept	The intercept of the regression trend line
Ratio (of median)	Median(O/M)

1.3 Example plots

In addition to the statistics, it is useful to visualize the validation results with various plots. Below are some example results from earlier validation work.

Scatter plots

Scatter plots visualize a dataset of in situ and EO data pairs (matchups). An example of a scatterplot can be seen in Figure 1. Often statistical measures are included in the plot to facilitate e.g. the comparison of different EO processing methods.

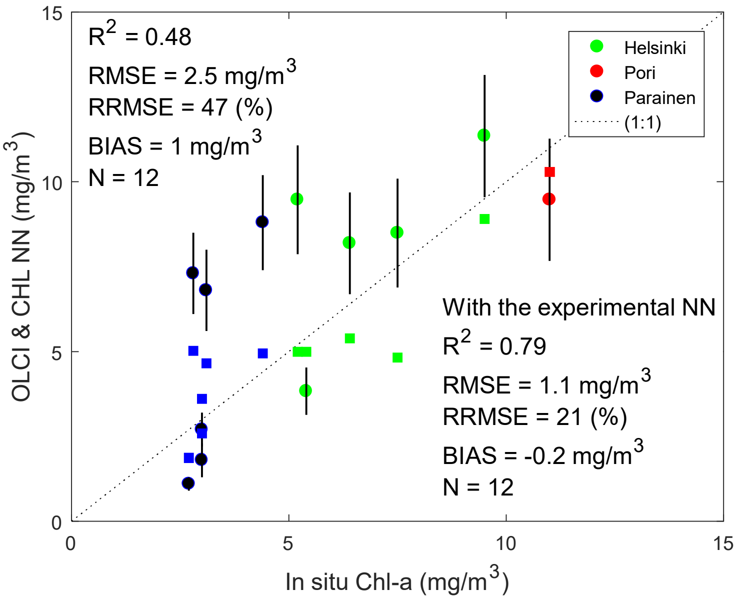

Figure 1. Example of a scatterplot. Chl-a estimated in the coastal areas of Finland with the standard C2RCC (circles; top left statistics) and with the experimental NN (squares; bottom right statistics). Image presented at Sentinel 3 Validation Team meeting, March 2018 by Sampsa Koponen.

Time series plots

Time series plots typically illustrate a dataset where the data has been collected multiple times from one location. The collection times of in situ and EO data may or may not be the same. The advantage of this is that dynamic behavior can be seen in both datasets even though the strictest requirements for the time difference of a matchup (see above) are not met. Figure 2 shows an example of this. Figure 3 in turn shows an example where EO and in situ data from a longer time period are visualized together. These may be useful in the open sea areas and with the model comparisons.

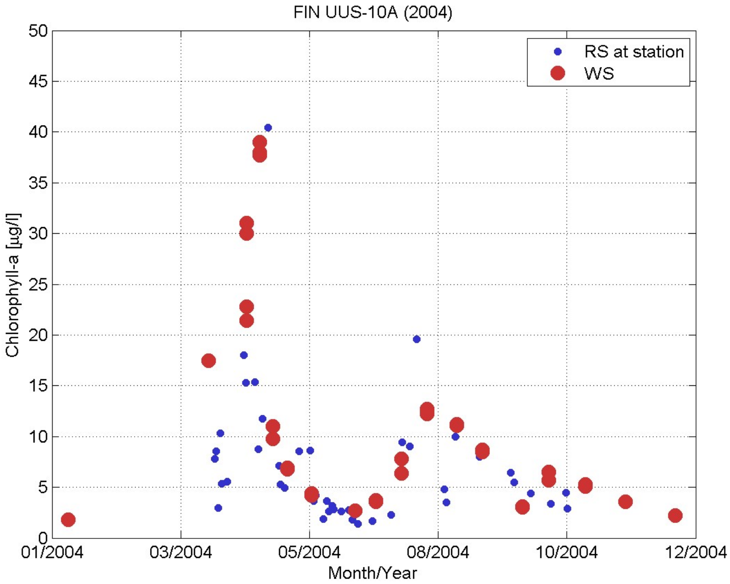

Figure 2. Example of a time series plot. Validation of MERIS Chl-a on an ICES station (HELCOM EUTRO-OPER, 2015).

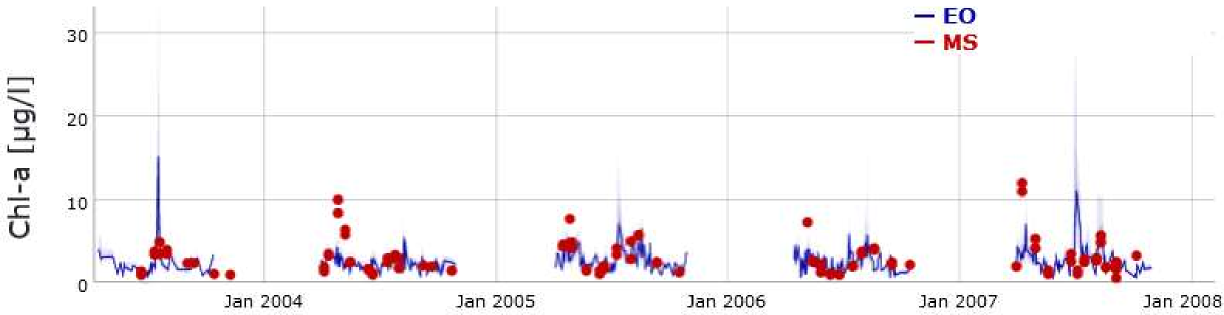

Figure 3. Example of a comparison of EO (MERIS & FUB processor) and monitoring station (MS) values aggregated within a 20 km by 20 km HELCOM grid.

Transect plots

Transect plots are made with in situ data collected from moving platforms (ships or boats). The main advantage of this is the possibility to collecting large amounts of data from a large area during a single campaign day. Figure 4 shows an example of this.

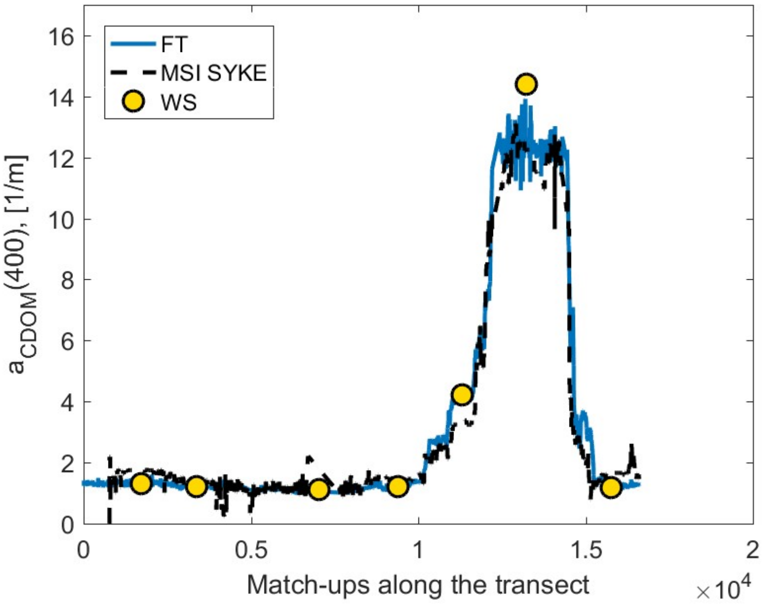

Figure 4. Example of a transect plot. Correspondence of the absorption of CDOM as analysed via S2 (MSI-SYKE, C2RCC-based algorithm,), field measured flow-through (FT) transect and water samples (WS) on a coastal estuary in Finland.

Product images

Product images show the concentrations of a water quality parameter as a map. The example in Figure 5 shows how a river causes elevated CDOM values in a coastal area during springtime due to the large amounts of dissolved material transported with water from melting snow.

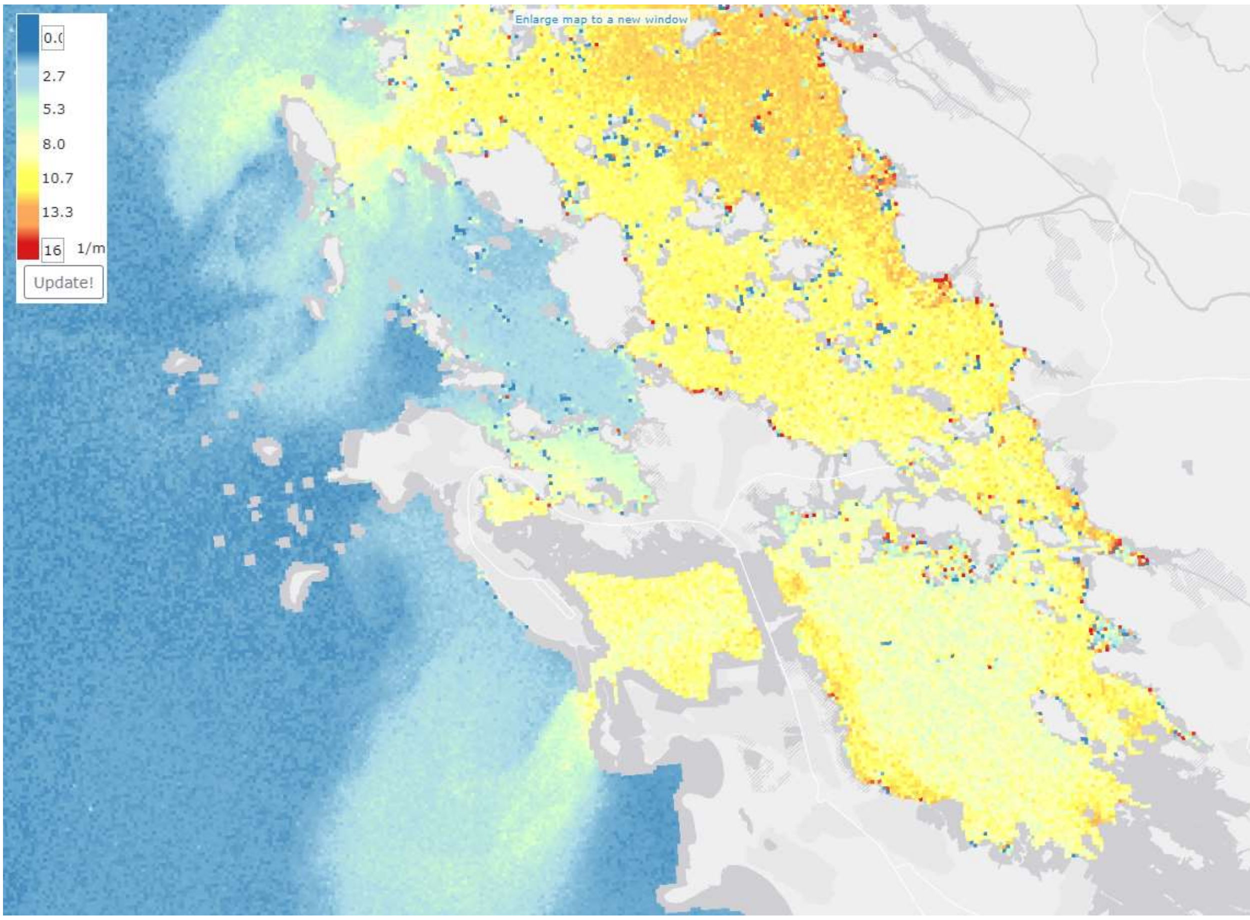

Figure 5. An example Sentinel-2 MSI C2RCC CDOM product from a river estuary in Western Finland on 2019-04-16.

2 Validation of atmospheric correction

2.1 Qualitative analysis on OLCI scenes

The Baltic+ AC has been tested on OLCI-A and OLCI-B scenes covering various water conditions: very absorbing waters in the North Gulf of Bothnia (Figure 6), brighter waters and turbid plumes near the estuary of the Kokemäenjoki river (Figure 7) and blue-green algae blooms in the Archipelago Sea (Figure 8). Results for POLYMER and C2RCC are also shown. In order to easily visualize the different level of radiometry (here at 443 nm), the same colour scale is used on all figures. Furthermore, this colour scale is also used for the Rayleigh corrected signal, ρ_{Rc}, and the aerosol signal identified by Baltic+, ρ_a. Comparison between ρ_{Rc}, ρ_a and ρ_w shows the challenges in decoupling the atmospheric and marine part.

Baltic+ AC manages to provide a smooth map of reflectance with realistic amplitude on the whole scenes. In the Gulf of Bothnia, the AC retrieves a very low, yet positive, signal at 443 nm. POLYMER fails and retrieves an erroneously high ρ_w in the most absorbing part, probably because of ambiguities between the aerosol and marine model not adapted for such cases. C2RCC performs relatively well but ρ_w appears quite high for this region, as confirmed in the analysis on match-ups.

All undetected clouds, visible on ρ_{Rc} map of Figure 7, are well corrected by the Baltic+ AC and POLYMER: their contribution is set to ρ_a, and the underlying marine reflectance looks realistic compared to the neighbouring pixels. On the contrary, these undetected clouds degrade performance of C2RCC, which underestimates ρ_w. This shows that the polynomial model from POLYMER, used in the Baltic+ AC, is robust to such contamination. On Figure 7, Baltic+ is providing the most contrasted map of reflectance, with relatively low value offshore (purples) while the plume is well captured, contrary to POLYMER. Still, it can be seen on the ρ_a map that the Baltic+ AC underestimates the aerosol on the most turbid parts of the plumes. We have observed that starting from other first guess could solve this issue. It is likely that the most complex situations could benefit from an improved backward NN, used as first guess, or possibly other tuning in the iterations.

Figure 8 shows an interesting case of OLCI camera interface, with a strong jump in radiometry, due to the well-known smile effect (non-homogenous detector wavelength inside each camera and between the cameras). The POLYMER and Baltic+ AC takes the exact wavelength of each pixels in the aerosol terms (as seen on map of ρ_a), and by subtraction the interface does not show any more on ρ_w. The interface in visible for C2RCC, whose NNs consider the same theoretical nominal wavelength for all pixels, and which would require a smile correction first. Aside from the camera interface, C2RCC presents also a noisy and high ρ_w. Baltic+ provides again the most contrasted map, with deep purple areas on most of the scene (ρ_w(443)<3*10^{-3}) but blooms clearly visible on the left-hand side of the scene.

Finally, the uncertainty map provided by the Baltic+ processor gives more insight in the trustworthiness of the inversion. Very high values appear in complex areas, like small inland waters, or in the most turbid part of the river plume. Interestingly, the uncertainty is not higher over the undetected clouds (except very limited pixels), what shows that the correction is as much trustable here as over other clear-sky adjacent pixels. In the north Gulf of Bothnia, the absolute level of uncertainty is very small, below 10^{-3}, which is a noticeable performance although it is relatively high compared to the extremely small amplitude of ρ_w. In general, the uncertainty level follows the amplitude of ρ_w, however not systematically: on Figure 7, in some part of the plume, and on Figure 8, in most of the algal bloom, the uncertainty remains as low as over less complex waters. The uncertainty relates strongly to the quality of the spectral fit, hence adequacy of the marine model, which is likely variable depending on IOPs. The uncertainty maps suggest trophic conditions where the model could be improved. In turn, the uncertainty of the marine model should, ideally, be used in the AC minimization, to constrain the bands with larger uncertainty. The current implementation technically allows for this capability but requires estimates of the forward model uncertainties, for a given set of IOPs. From general behaviour of non-linear least-square minimization, it can be expected that constraining the inversion with input uncertainties will reduce the amplitude of the output uncertainty.

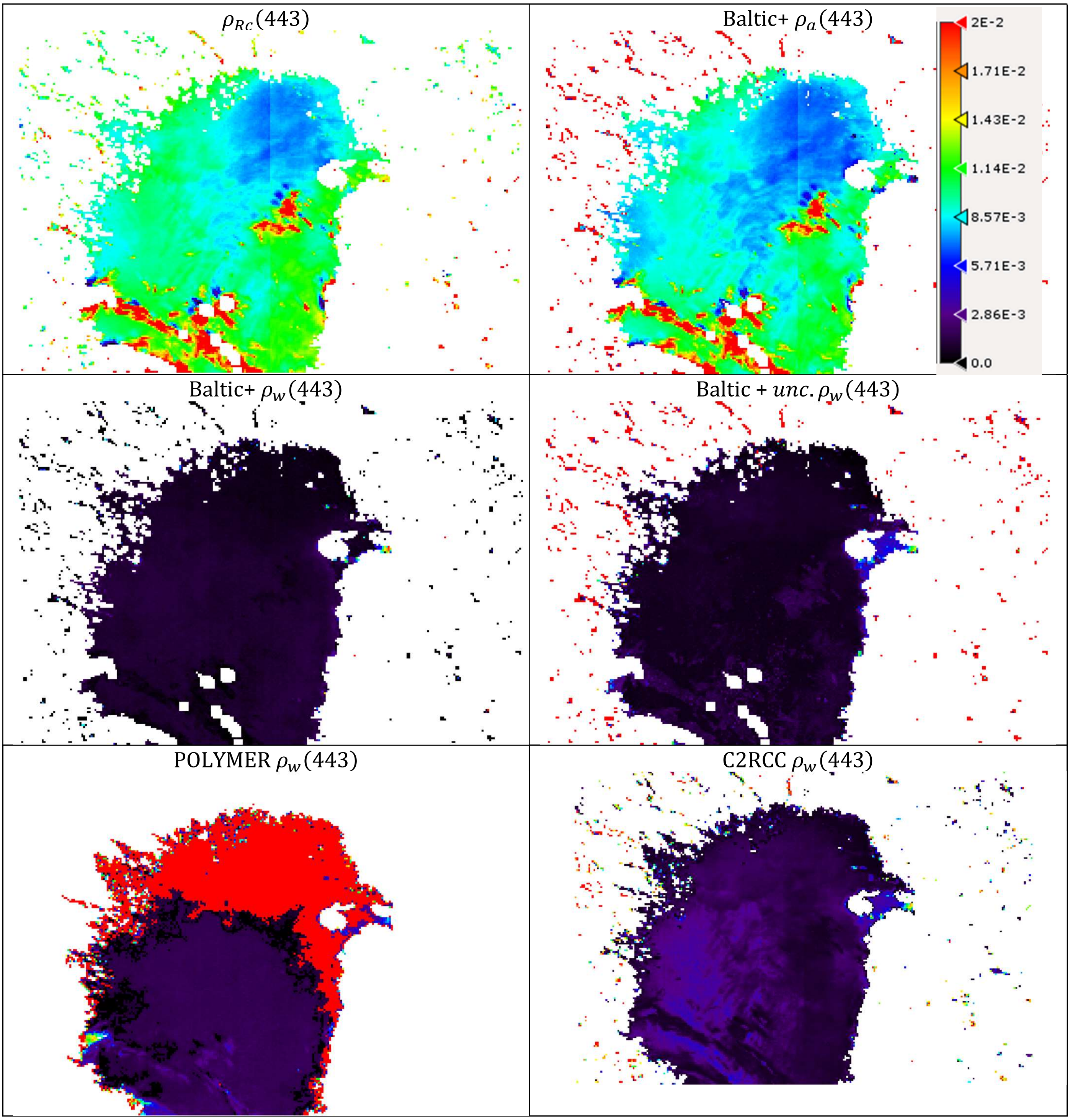

Figure 6 Analysis of Baltic+ AC in northern Gulf of Bothnia (OLCI-A, 20180602). Same colour scale for ρ_{Rc}, ρ_w and $unc.\,\rho_w$ (top right colour bar). Band 443 nm.

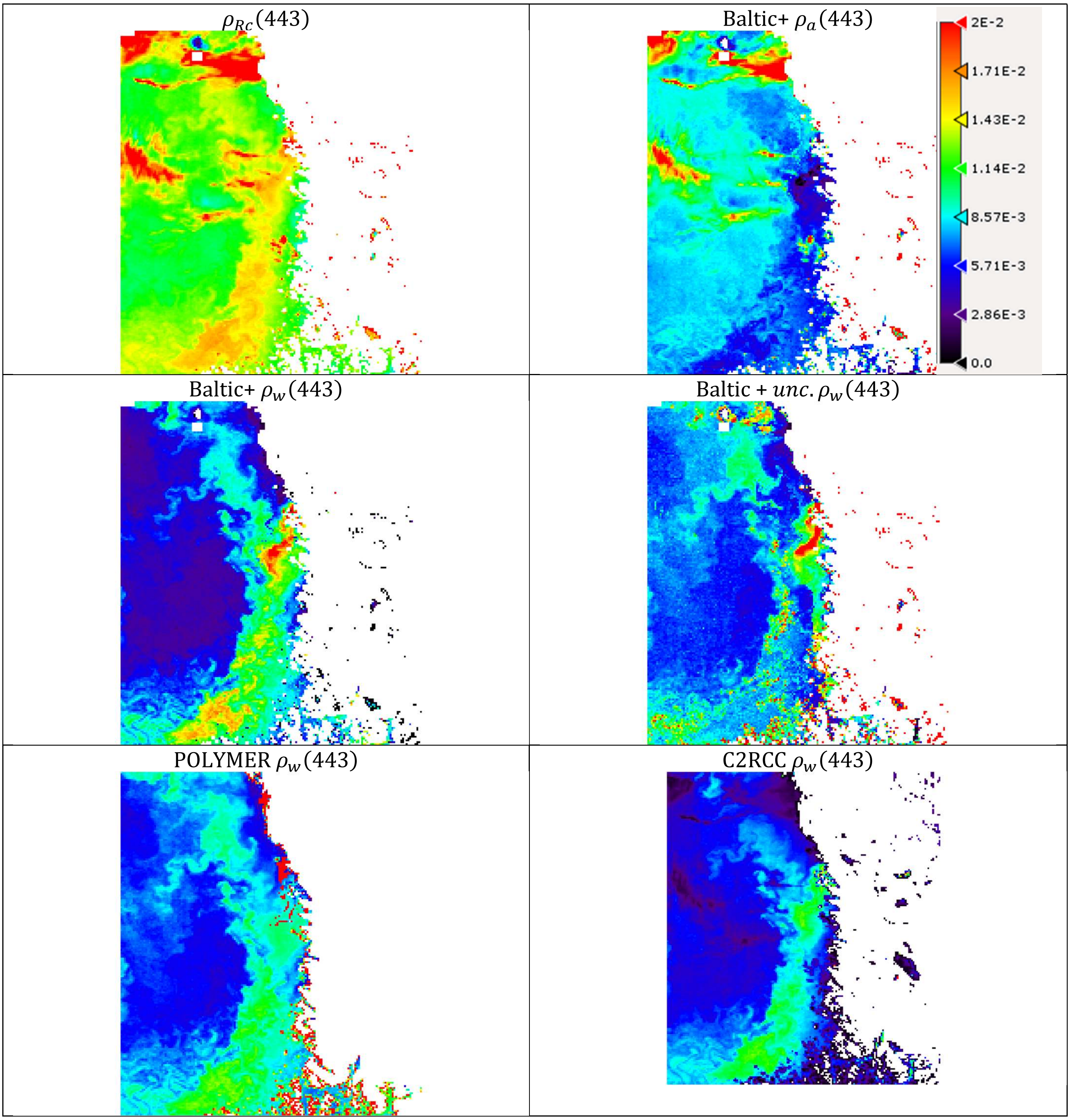

Figure 7 Analysis of Baltic+ AC on the estuary of the Kokemäenjoki river (OLCI-B, 20190415. Same colour scale for ρ_{Rc}, ρ_w and $unc.\rho_w$ (top right colour bar). Band 443 nm.

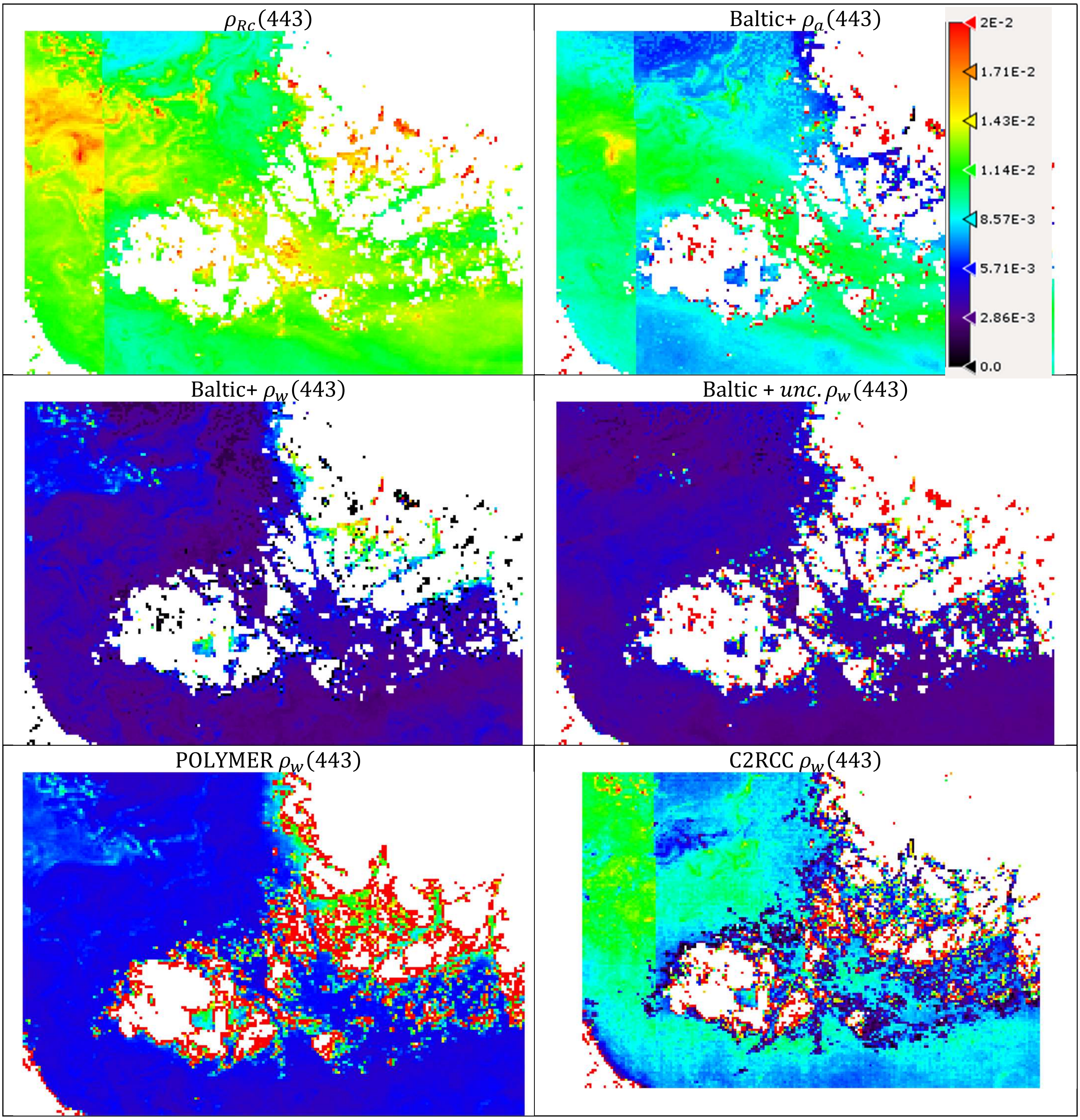

Figure 8 Analysis of Baltic+ AC in the Archipelago Sea (OLCI-A, 20170814). Same colour scale for ρ_{Rc}, ρ_w and $unc.\rho_w$ (top right colour bar). Band 443 nm.

2.2 OLCI-A match-ups

In Figure 9 and Figure 10 we compare the OLCI-A normalized reflectances provided by the Baltic AC processor (version with forward NN) and other processors (POLYMER (Steinmetz et al., 2011), C2RCC (Brockmann et al., 2016) and standard AC (IPF; Antoine and Morel, 1999)) against the normalized reflectance measurements from the AERONET-OC stations in the Baltic (Gustav Dalen Tower, Helsinki Lighthouse) and in a lake in Sweden (Palgrunden). The processing includes all S3 match-ups available from May 2016 to June 2017. The analysis is limited to standard AERONET-OC bands, i.e. 412, 443, 490, 510, 560 and 665 nm which benefit from highest quality assurance (Zibordi et al., 2009); according to the PI (G. Zibordi, JRC,) AERONET-OC measurements further in the NIR, at 865 and 1020 nm, are of lower quality and not suited for validation: "Additional measurements are performed at 709, 865, and 1020 nm for quality checks, turbid water flagging, and for the application of alternative above-water method" (https://aeronet.gsfc.nasa.gov/new_web/ocean_levels_versions.html). Note that the number of match-ups may vary with wavelengths due to lack of in situ measurements, especially at 510 and 560 nm.

The screening criteria applied on the match-ups follows standard protocols in ocean colour radiometry (Bailey and Werdell, 2006):

- Maximum time difference between in situ and satellite acquisitions of 3 hours
- 50% of valid pixels in the micro-pixels (here 15x15 FR pixels), depending on quality flags
- Outlier removal in the averaging (pixels whose value differ from the mean by more than 1.5 std-dev)
- Coefficient of Variation (std-dev / mean) lower than 0.2

Flags depend on the processor as follows:

- Currently, the Baltic+ processor does not provide quality flags, although uncertainties are available (vertical lines in next plot; only available for Baltic+). Furthermore, the classification by Idepix could not be applied upstream of the Baltic+ match-ups processing (whereas it can be for scenes processing), making the data possibly impacted by clouds. Despite this absence of flagging, the screening only based on statistical filtering seems to be enough to remove dubious data.
- For C2RCC, the flags are: Rtosa_OOS, Rtosa_OOR, Rhow_OOR, Rhow_OOS, Cloud_risk
- For POLYMER, the flag is “bitmask & 1023” (standard flagging used for instance in ESA OC-CCI)
- For the IPF, we apply the flags recommended in the Sentinel-3 Validation Team protocols: INVALID, AC_FAIL, WHITECAPS, ANNOT_ABSO_D, ANNOT_MIXR1, ANNOT_TAU06 and RWNEG from band 2 to band 8. The number of valid data appears to be very low. We have checked that removing these flags would add few more points, but would not help to reach the numbers available by other processors.

The results show that the standard processor (IPF) is not doing well in the blue (412 nm) whereas the performance is good at other bands (560, 665 nm) for the very few stations passing the criteria. The big issue for IPF is the number of available data points, much smaller than with the other processors. C2RCC is doing better, with much more data and good performance in the red, but it also has overestimation problems in the blue and green parts of the spectrum, together with scattered data. The results with POLYMER are very good in term of number of valid data and overall bias, despite overestimation in the blue too. At 412 nm, the Baltic processor yields the best regression slope (about 0.80) and lowest absolute bias of about $2*10^{-3}$. Baltic+ has the best regression coefficient (around 0.8, except at 412 nm), indicating robust results, but there is a slope from 490 nm not observed for other ACs. We have observed that the results on match-ups depends significantly on the first guess of the minimization, currently given by a backward NN; other options can improve the results. Since the current backward NN is known to have limitation (in particular the use of 1020 nm, affected by strong calibration issue), we can expect improved results with a future version of this NN.

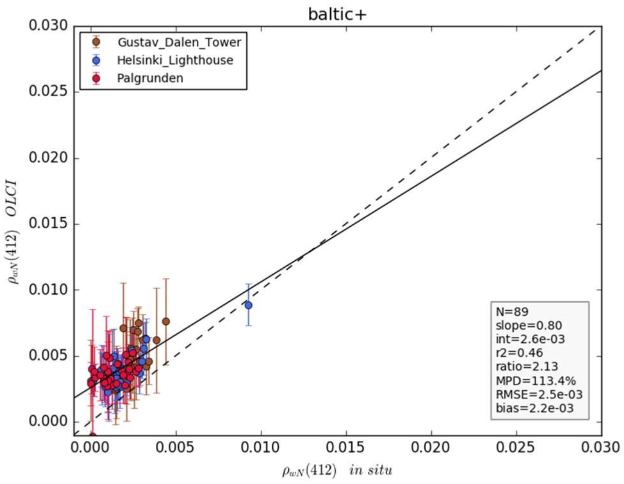
baltic+
Gustav_Dalen_Tower
Helsinki_Lighthouse
Palgrunden
N=89
slope=0.80
int=2.6e-03
r2=0.46
ratio=2.13
MPD=113.4%
RMSE=2.5e-03
bias=2.2e-03
$\rho_{wN}(412)$ OLCI
$\rho_{wN}(412)$ in situ

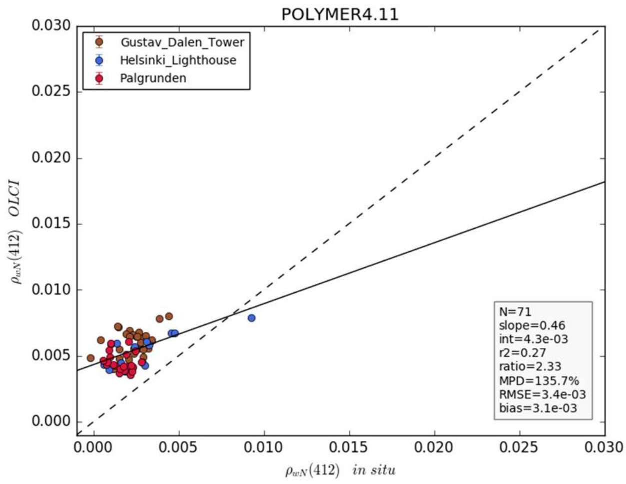
POLYMER4.11
Gustav_Dalen_Tower
Helsinki_Lighthouse
Palgrunden
N=71
slope=0.46
int=4.3e-03
r2=0.27
ratio=2.33
MPD=135.7%
RMSE=3.4e-03
bias=3.1e-03
$\rho_{wN}(412)$ OLCI
$\rho_{wN}(412)$ in situ

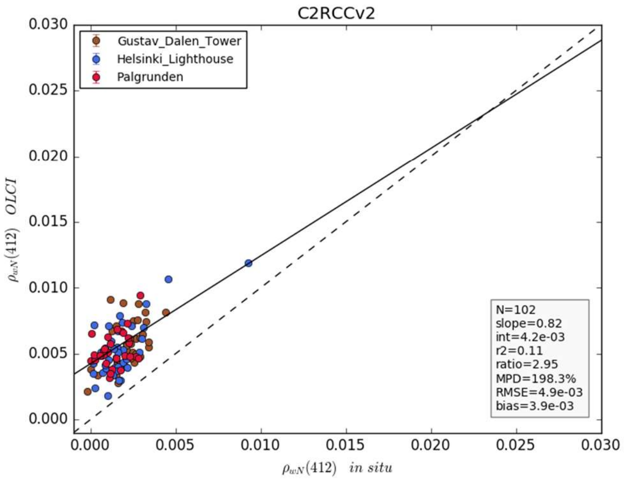
C2RCCv2
Gustav_Dalen_Tower
Helsinki_Lighthouse
Palgrunden
N=102
slope=0.82
int=4.2e-03
r2=0.11
ratio=2.95
MPD=198.3%
RMSE=4.9e-03
bias=3.9e-03
$\rho_{wN}(412)$ OLCI
$\rho_{wN}(412)$ in situ

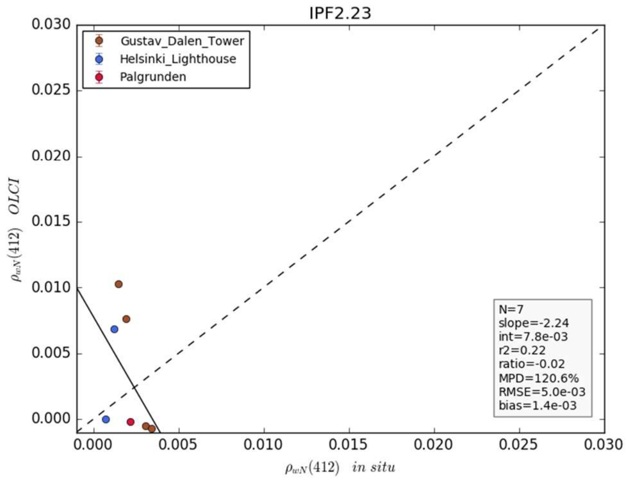
IPF2.23
Gustav_Dalen_Tower
Helsinki_Lighthouse
Palgrunden
N=7
slope=-2.24
int=7.8e-03
r2=0.22
ratio=-0.02
MPD=120.6%
RMSE=5.0e-03
bias=1.4e-03
$\rho_{wN}(412)$ OLCI
$\rho_{wN}(412)$ in situ

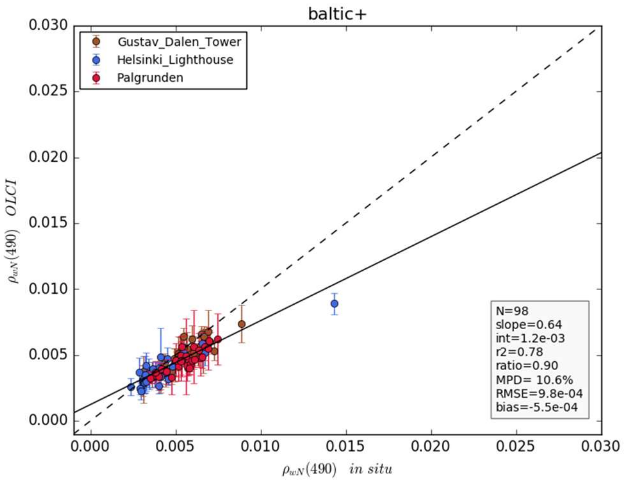
baltic+
Gustav_Dalen_Tower
Helsinki_Lighthouse
Palgrunden
N=98
slope=0.64
int=1.2e-03
r2=0.78
ratio=0.90
MPD= 10.6%
RMSE=9.8e-04
bias=-5.5e-04
$\rho_{wN}(490)$ OLCI
$\rho_{wN}(490)$ in situ

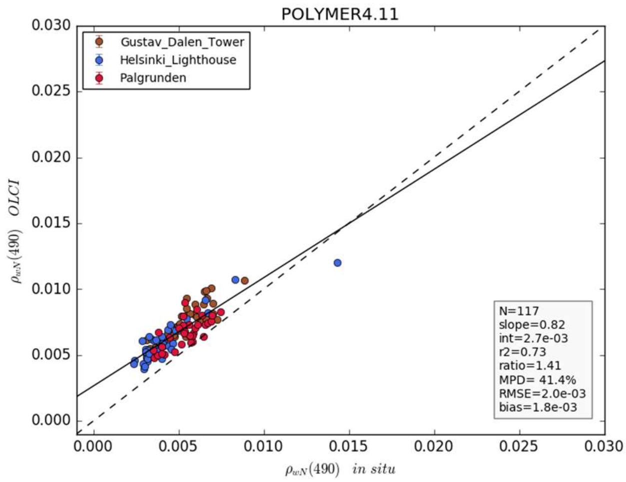
POLYMER4.11
Gustav_Dalen_Tower
Helsinki_Lighthouse
Palgrunden
N=117
slope=0.82
int=2.7e-03
r2=0.73
ratio=1.41
MPD= 41.4%
RMSE=2.0e-03
bias=1.8e-03
$\rho_{wN}(490)$ OLCI
$\rho_{wN}(490)$ in situ

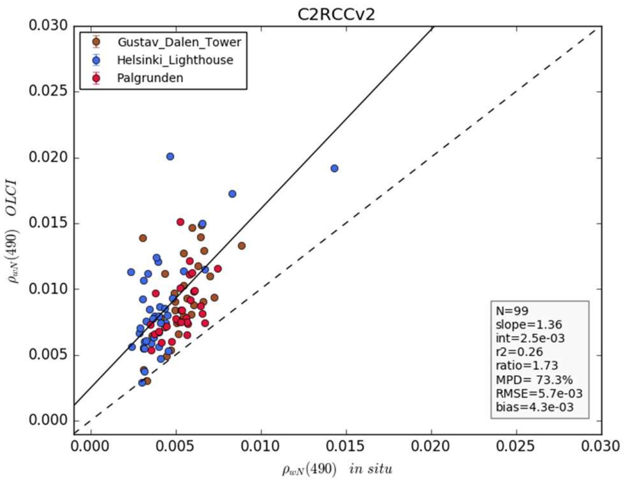
C2RCCv2
Gustav_Dalen_Tower
Helsinki_Lighthouse
Palgrunden
N=99
slope=1.36
int=2.5e-03
r2=0.26
ratio=1.73
MPD= 73.3%
RMSE=5.7e-03
bias=4.3e-03
$\rho_{wN}(490)$ OLCI
$\rho_{wN}(490)$ in situ

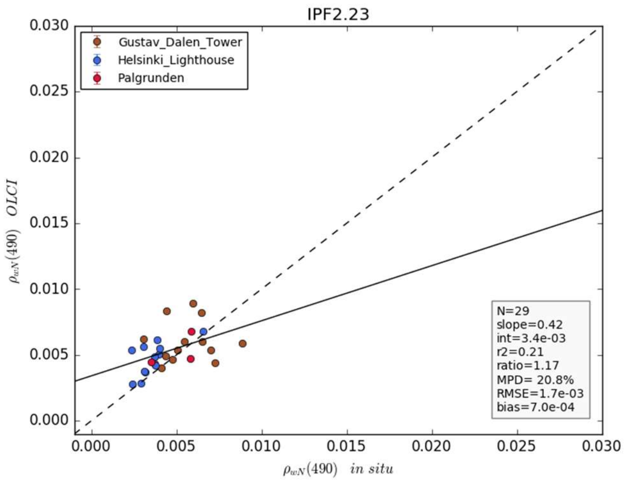
IPF2.23
Gustav_Dalen_Tower
Helsinki_Lighthouse
Palgrunden
N=29
slope=0.42
int=3.4e-03
r2=0.21
ratio=1.17
MPD= 20.8%
RMSE=1.7e-03
bias=7.0e-04
$\rho_{wN}(490)$ OLCI
$\rho_{wN}(490)$ in situ

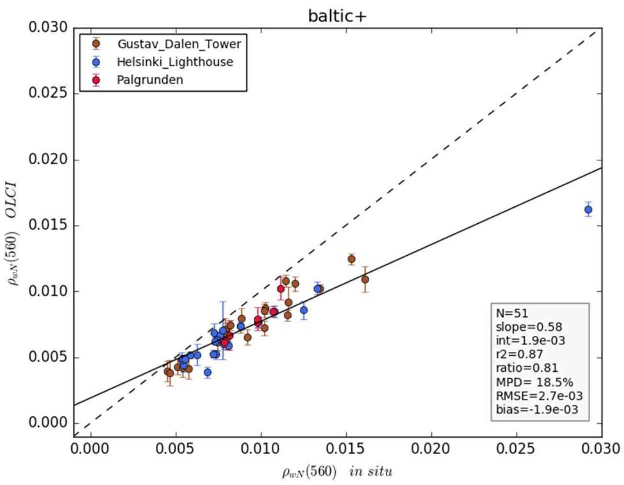
baltic+
Gustav_Dalen_Tower
Helsinki_Lighthouse
Palgrunden
N=51
slope=0.58
int=1.9e-03
r2=0.87
ratio=0.81
MPD= 18.5%
RMSE=2.7e-03
bias=-1.9e-03
$\rho_{wN}(560)$ OLCI
$\rho_{wN}(560)$ in situ

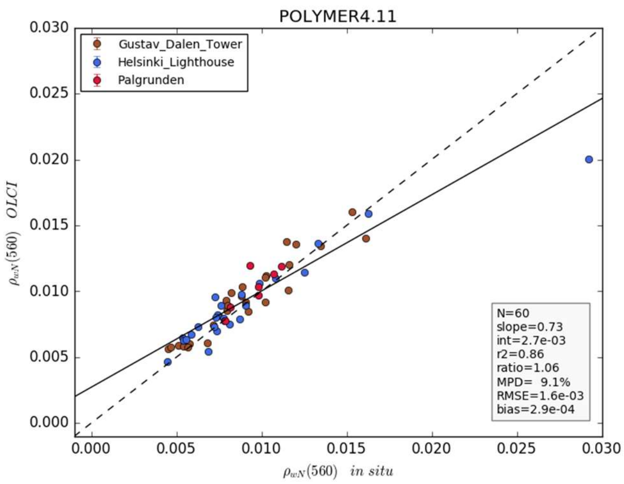
POLYMER4.11
Gustav_Dalen_Tower
Helsinki_Lighthouse
Palgrunden
N=60
slope=0.73
int=2.7e-03
r2=0.86
ratio=1.06
MPD= 9.1%
RMSE=1.6e-03
bias=2.9e-04
$\rho_{wN}(560)$ OLCI
$\rho_{wN}(560)$ in situ

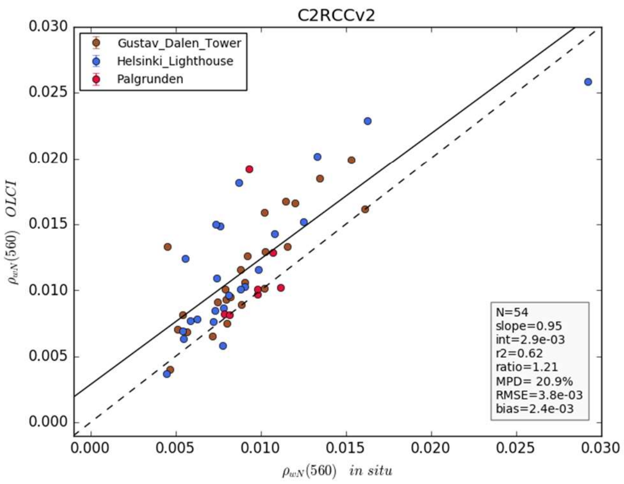
C2RCCv2
Gustav_Dalen_Tower
Helsinki_Lighthouse
Palgrunden
N=54
slope=0.95
int=2.9e-03
r2=0.62
ratio=1.21
MPD= 20.9%
RMSE=3.8e-03
bias=2.4e-03
$\rho_{wN}(560)$ OLCI
$\rho_{wN}(560)$ in situ

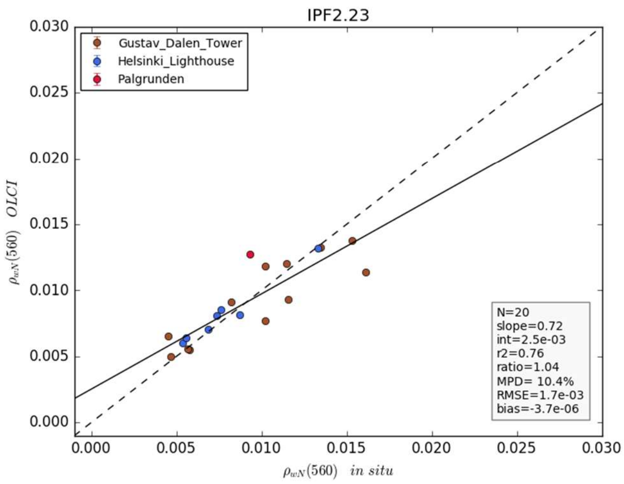
IPF2.23
Gustav_Dalen_Tower
Helsinki_Lighthouse
Palgrunden
N=20
slope=0.72
int=2.5e-03
r2=0.76
ratio=1.04
MPD= 10.4%
RMSE=1.7e-03
bias=-3.7e-06
$\rho_{wN}(560)$ OLCI
$\rho_{wN}(560)$ in situ

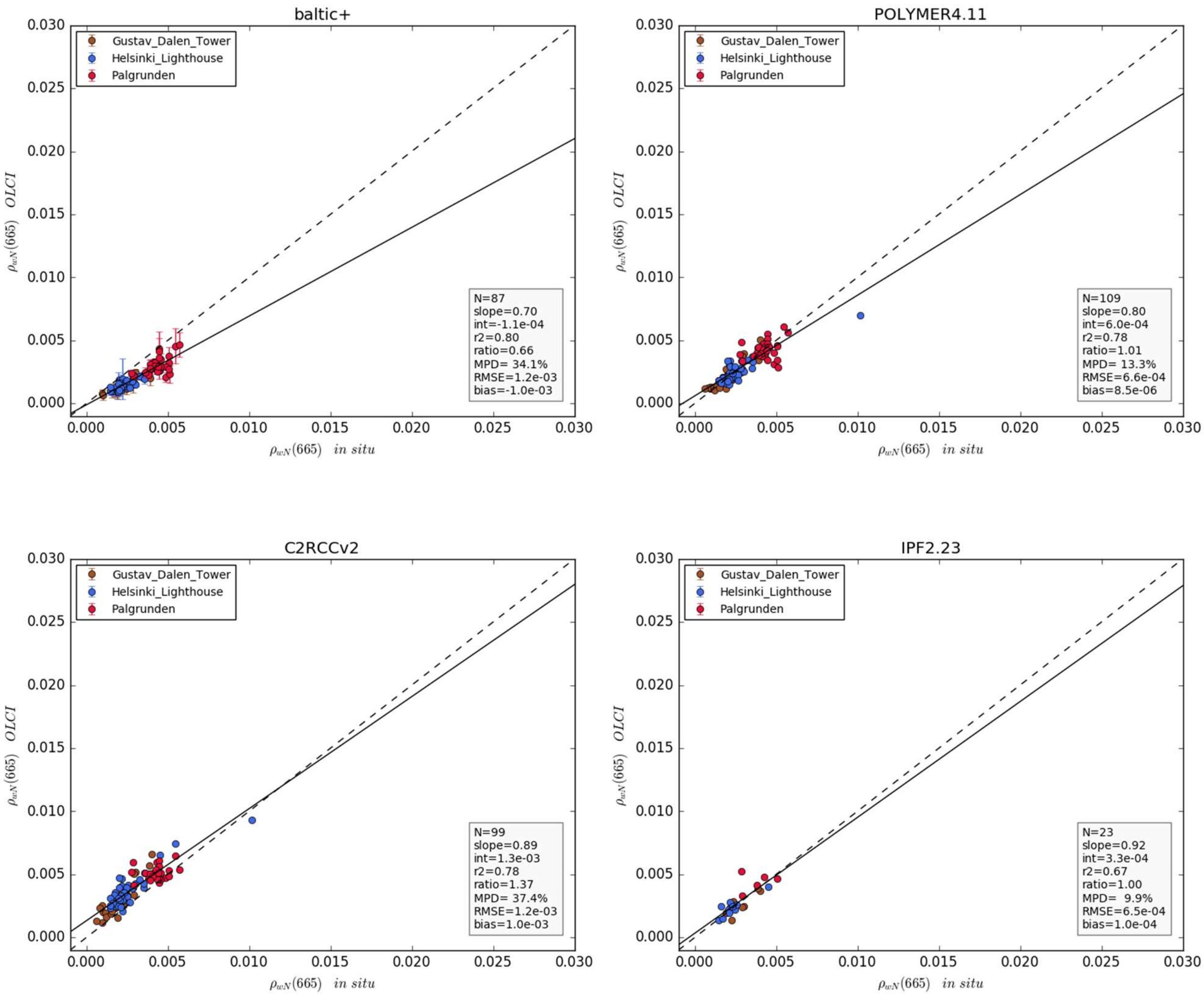

Figure 9. Comparisons of ρ_{wN} values provided by the Baltic+, C2RCC, POLYMER and IPF processors (with Sentinel 3 data) and in situ ρ_{wN} measured at Aeronet OC stations (Gustav Dalen Tower, Helsinki Lighthouse and Palgrunden) at 412 nm, 490 nm, 560 nm and 665 nm. For Baltic+, vertical lines correspond to the estimated uncertainties in marine reflectance.

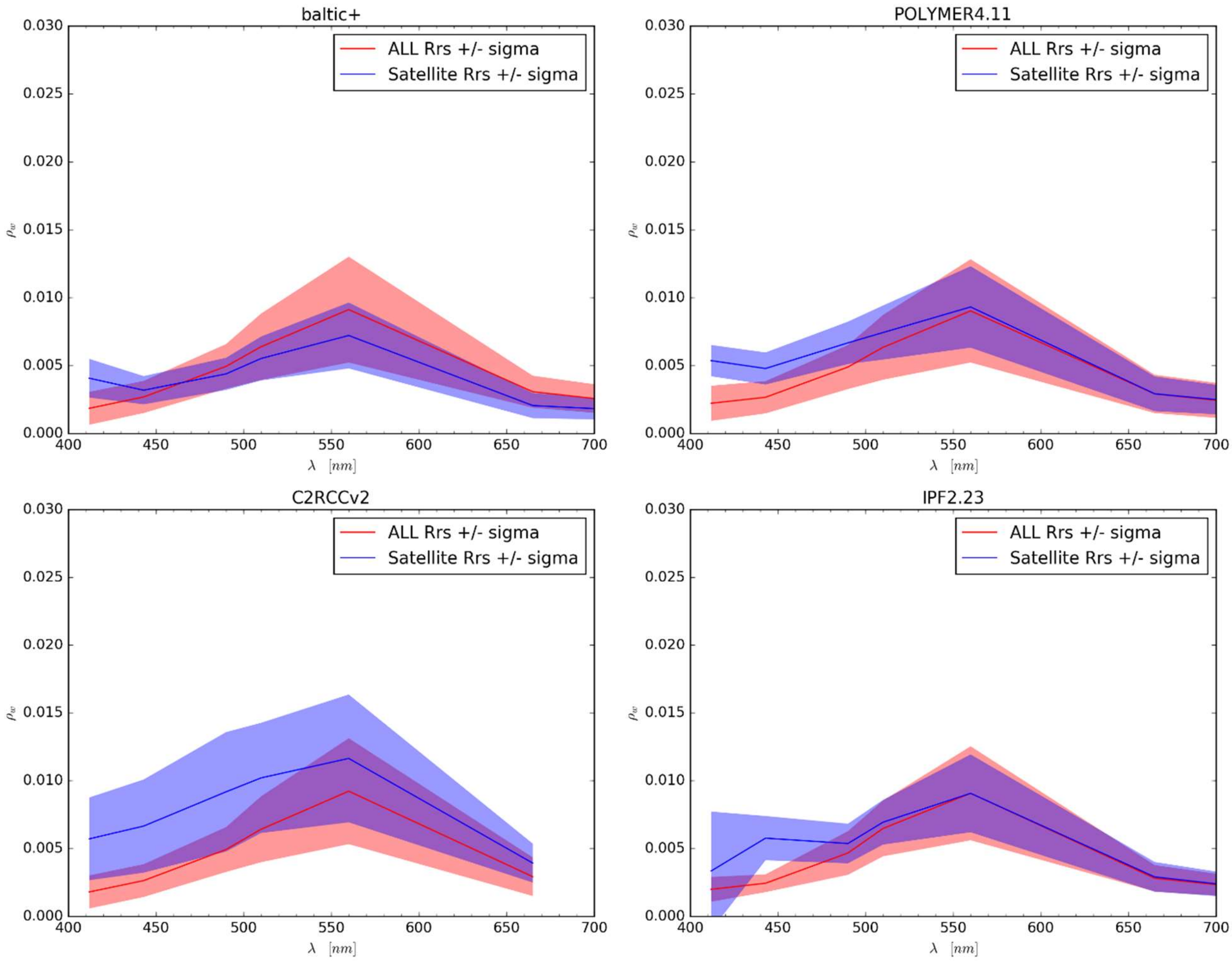

Figure 10. Averaged spectra of ρ_{wN} provided by the Baltic+, C2RCC, POLYMER and IPF processors (with Sentinel 3 data, in blue) and compared to in situ ρ_{wN} measured at AERONET-OC stations (Gustav Dalen Tower, Helsinki Lighthouse, Plagrunden, in red).

2.3 Validation plans

The AC has been adapter for S2. Specific pre-processing parts have been implemented. The core part of the code is the inversion which is common to S3 and S2. Performance of the AC using forward NN is not ensured for S2, due to the limited number of bands compared to the 5 IOPs to inverse: forwardNN for S2 provides marine reflectance at eight bands only (443, 490, 560, 665, 705, 740, 783, 865 nm), versus 14 bands used for OLCI. Validation of S2 data is thus currently postponed.

3 Validation of in-water parameters

3.1 Sentinel-2 & C2RCC

We tested the use of Sentinel-2 data processed with C2RCC V1 processor for providing aCDOM data for the purposes of this project (see the Dataset User Manual deliverable for more details). This product has been calibrated with data from Finnish coastal campaigns and routine monitoring measurements (see e.g. Figure 4) and works well in the Finnish conditions. For example, Figure 11 shows the behavior of EO data against in situ measurements at two coastal stations in the Bay of Bothnia. Both datasets show a clear seasonal cycle and the EO interpretation follows well the in-situ values.

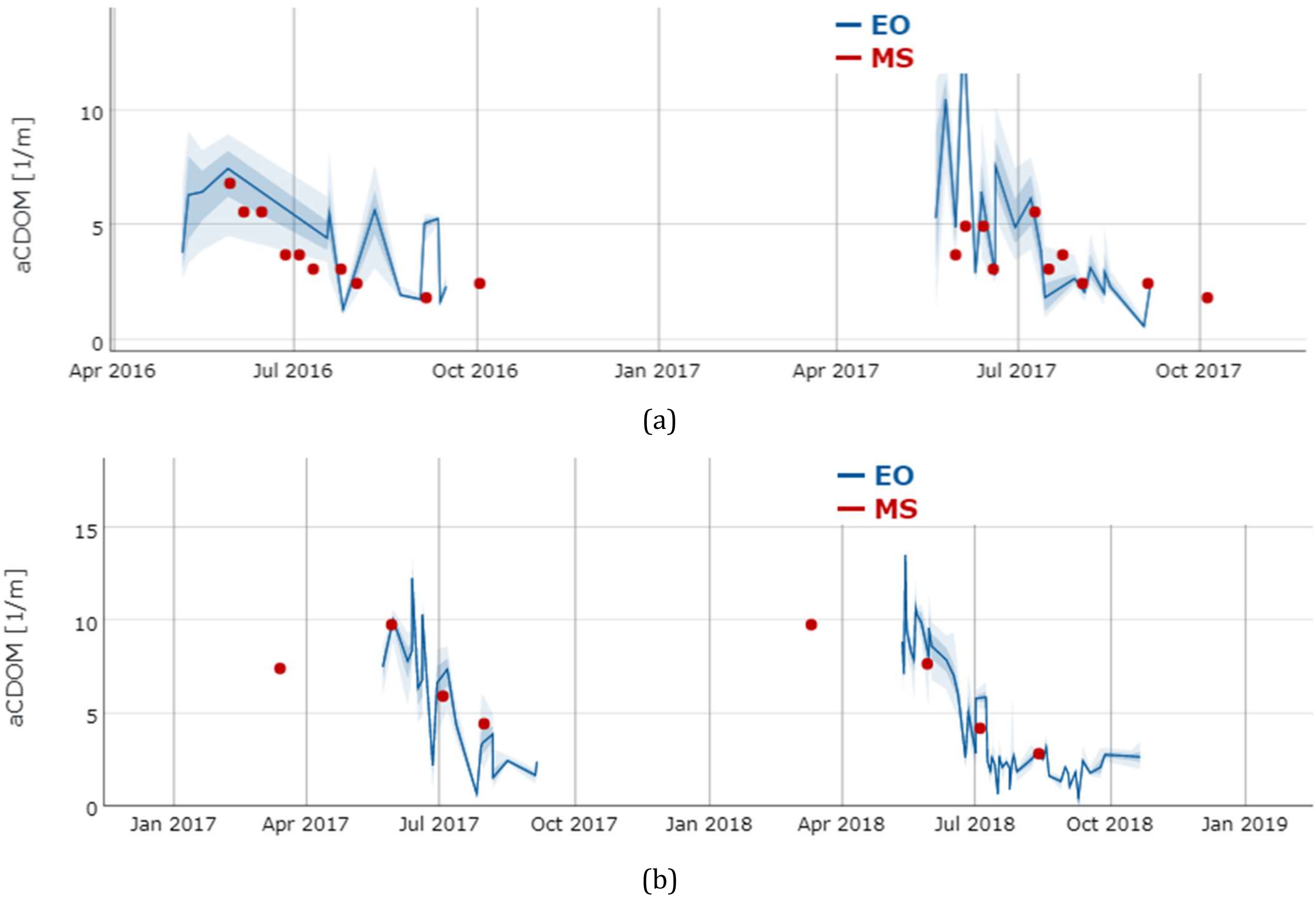

Figure 11. aCDOM derived from Sentinel-2 data with C2RCC V1 processor vs. in situ values measured at (a) the Hailuoto intensive monitoring station and (b) Luodonselkä station (both located at the Northern end of the Baltic Sea). The wavelength of the aCDOM determination is 400 nm. The images were extracted from SYKE's TARKKA service.

The S2 processing line was validated with the in situ data collected in WP2 (Dataset). aCDOM in situ measurements were only available from Finland and Sweden. The matchups represent the mean of 5 by 5 pixel areas (60 m pixels) using same day data. The results are shown in Figure 12 while Figure 13 shows the locations of the matchup stations. Figure 12 includes results for the data calibrated for Finland and the direct output of the processor. The coefficient of determination is about 0.5, which is quite good. There is a fair amount of scatter as shown by the RMSE values. Nevertheless, this processing line can provide sufficiently good CDOM data for the ERGOM model.

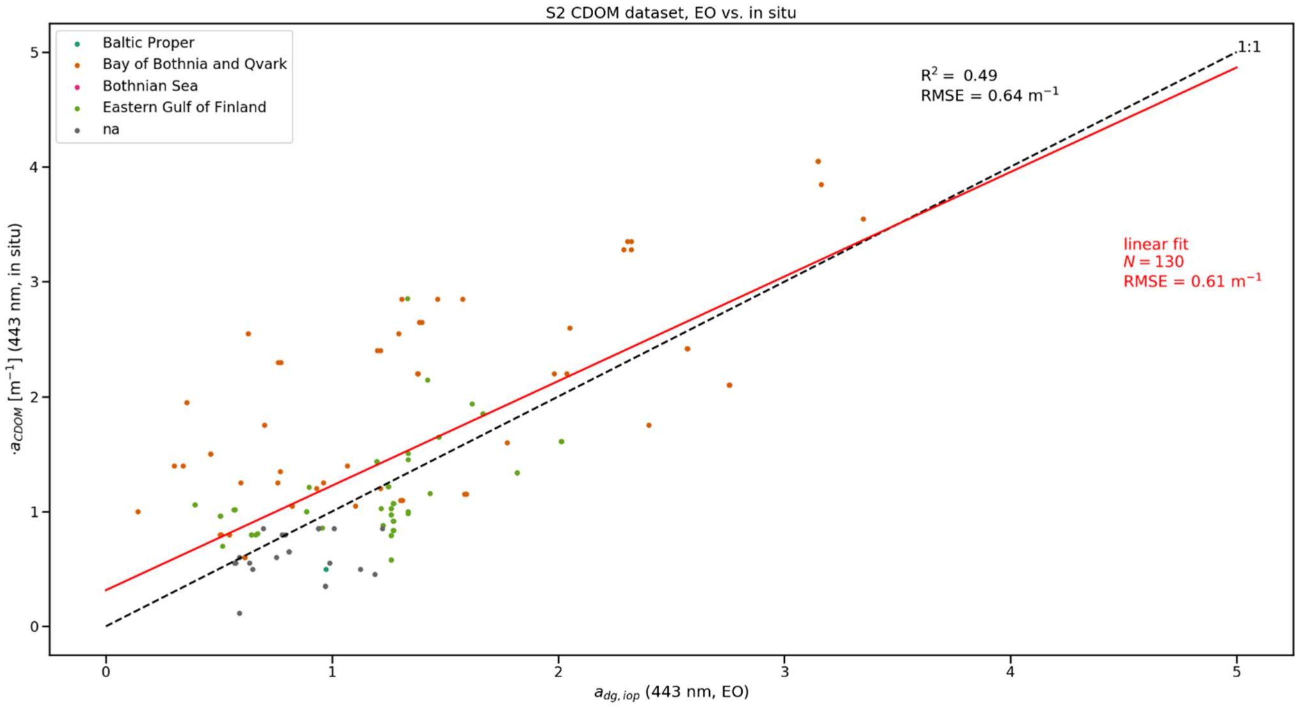

(a)

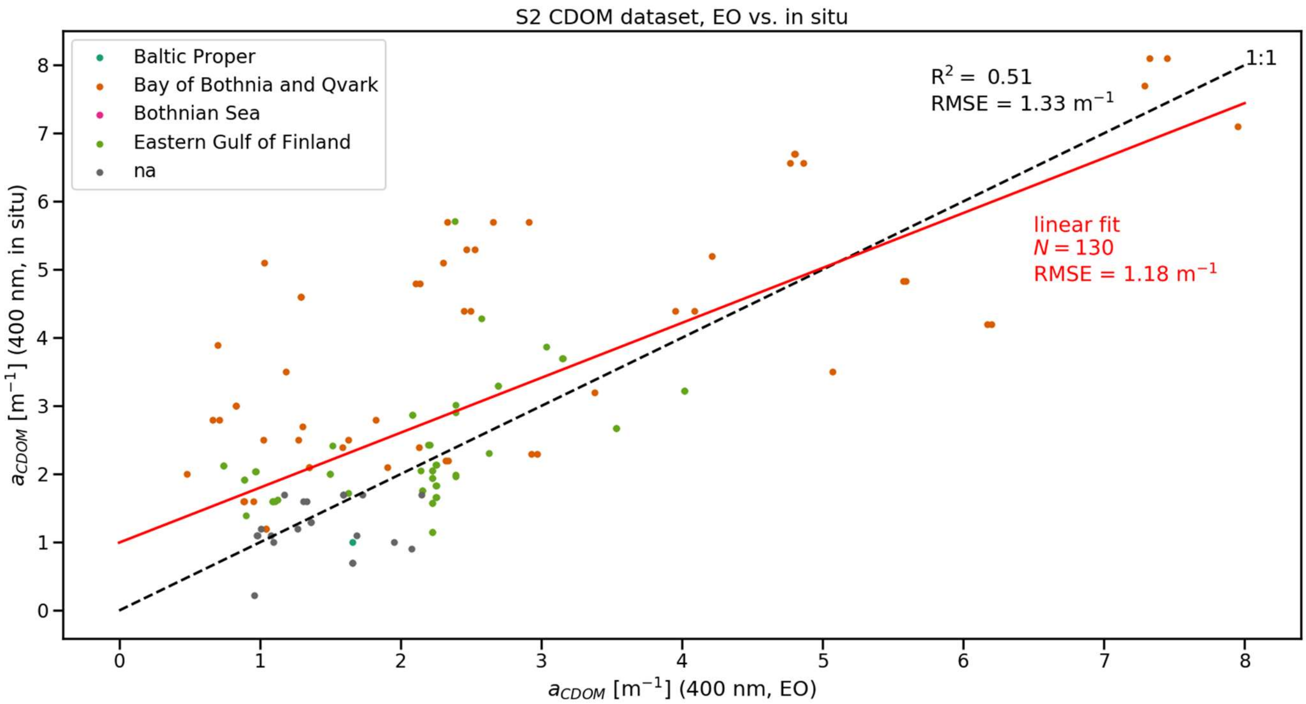

(b)

Figure 12. aCDOM derived from Sentinel-2 data with C2RCC V1 processor vs. in situ values from monitoring stations. In (a) the processor output (a_dg) is used directly while in (b) the processor output has been calibrated with in situ data from Finland. Note that the wavelength used in the CDOM absorption coefficient in the sub-figures are different.

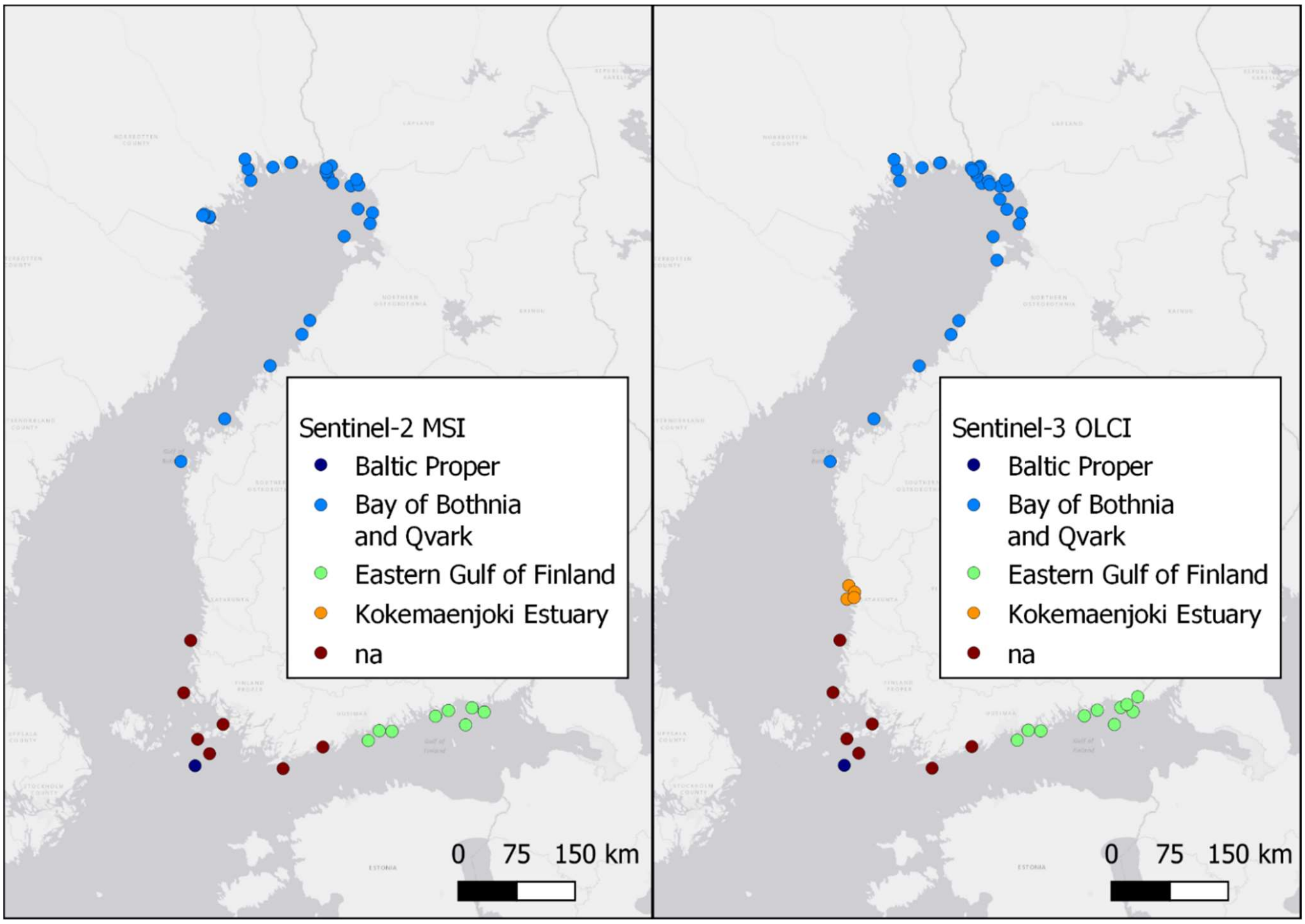

Figure 13. Locations of the matchup stations.

Band ratio algorithms were also tested to derive CDOM from atmospherically corrected reflectances. According to the simulations (Figure 14) it is possible to use a ratio of bands in red and green wavelengths with S2 MSI data. This has the advantage of avoiding the blue wavelengths where atmospheric correction algorithms often have problems and the signal can be low (especially in high CDOM situations). Figure 15 shows the result with Rhown bands derived from S2 data with the C2RCC V1 processor. According to these results the ratio B4/B3 (665 nm and 560 nm, respectively) gives the bests correlation followed by B5/B3 (709 nm and 560 nm, respectively).

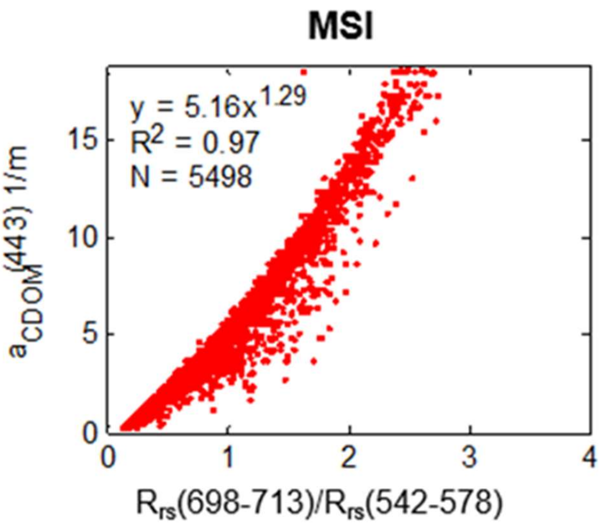

Figure 14. Band ratio algorithm for aCDOM based on HydroLight simulations made from concentrations found in Finnish lakes (Kallio et al. 2014).

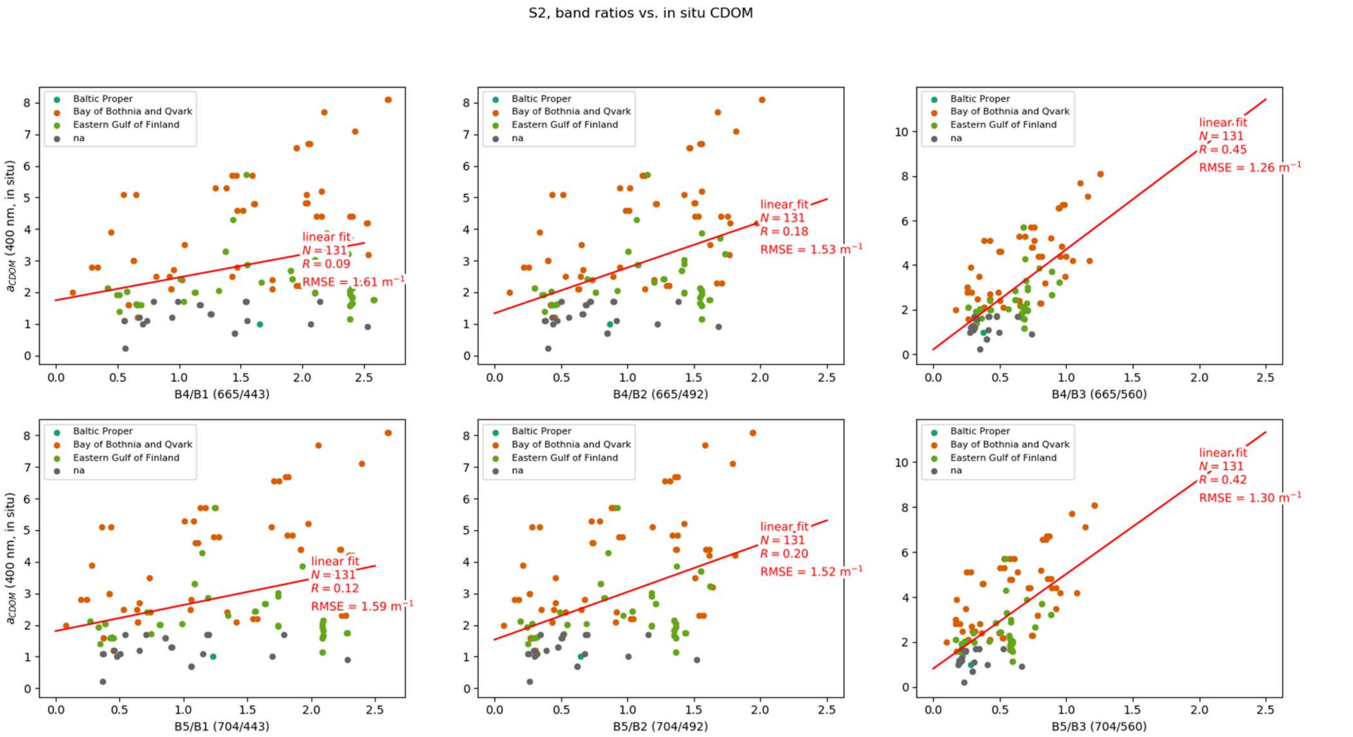

Figure 15. Sentinel-2 & C2RCC V1 reflectance band ratios vs. in situ aCDOM. Note that the wavelength used in the CDOM absorption coefficient is 400 nm.

3.2 Sentinel-3 OLCI & C2RCC

Sentinel-3 OLCI data were processed to matchups with C2RCC V1 similarly to Sentinel-2 data (Chapter 3.1). However, this processing line has not been calibrated with the Finnish in situ data and hence only the raw processor output (a_dg) is compared against in situ data. The matchups were formed from same day data but with 3 by 3 macro pixels. The results are shown in Figure 16 and matchup locations in Figure 13. Figure 17 shows the results with band ratios. These results are clearly worse than with S2 data. The number of matchups is larger than with S2 data due to the better temporal coverage.

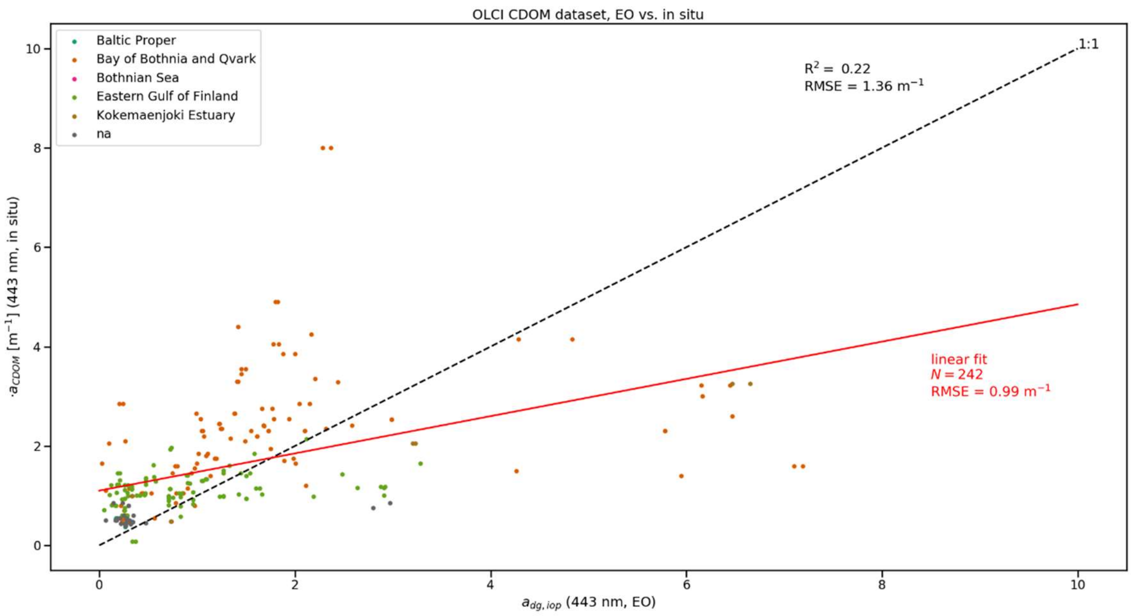

Figure 16. aCDOM derived from Sentinel-3 OLCI data with C2RCC V1 processor (a_dg) vs. in situ values from monitoring stations. Note that the wavelength used in the CDOM absorption coefficient is 443 nm.

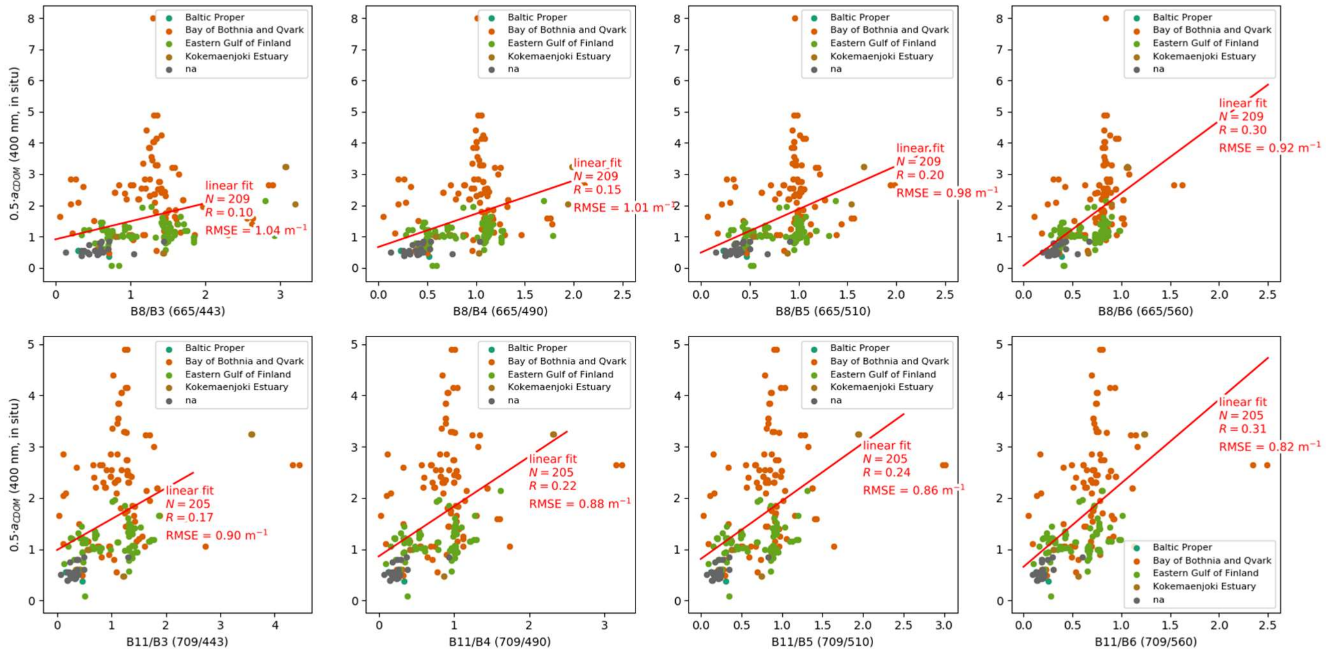

Figure 17. Sentinel-3 & C2RCC V1 reflectance band ratios vs. in situ aCDOM. Note that the wavelength used in the CDOM absorption coefficient is 443 nm.

3.3 Sentinel-3 OLCI & Baltic+ AC

The final test was the matchup analysis with OLCI data and the new Baltic+ AC processor (Figure 18). With reflectance band ratios there is a clear improvement in correlation compared to the C2RCC. Here 5*5 macro-pixels were used and any macro-pixel with less than 20 valid pixels were not included in the analysis. The best correspondences were found with band ratios B8/B6 and B11/B6. For further analysis the ratio B8/B6 was selected since B11 (709 nm) still had some uncertainties in the aerosol estimation. B6 is the 560 nm band. The calibration equation for this case is:

$$a_{CDOM}(400nm) = 4.85 * \left(\frac{\rho_{wn}(665nm)}{\rho_{wn}(560nm)}\right) + 0.65 \tag{3.1}$$

Figure 19 shows the aCDOM time series plot of a station located in the Finnish side of the Bay of Bothnia (Northern Baltic Sea) when Eq. (3.1) has been used in the processing of OCLI data. The EO result follow well the behavior of the in situ data although some overestimations remain in the low in situ values. The EO result contains some variations which may be noise. Thus, the use of temporal aggregation is recommended.

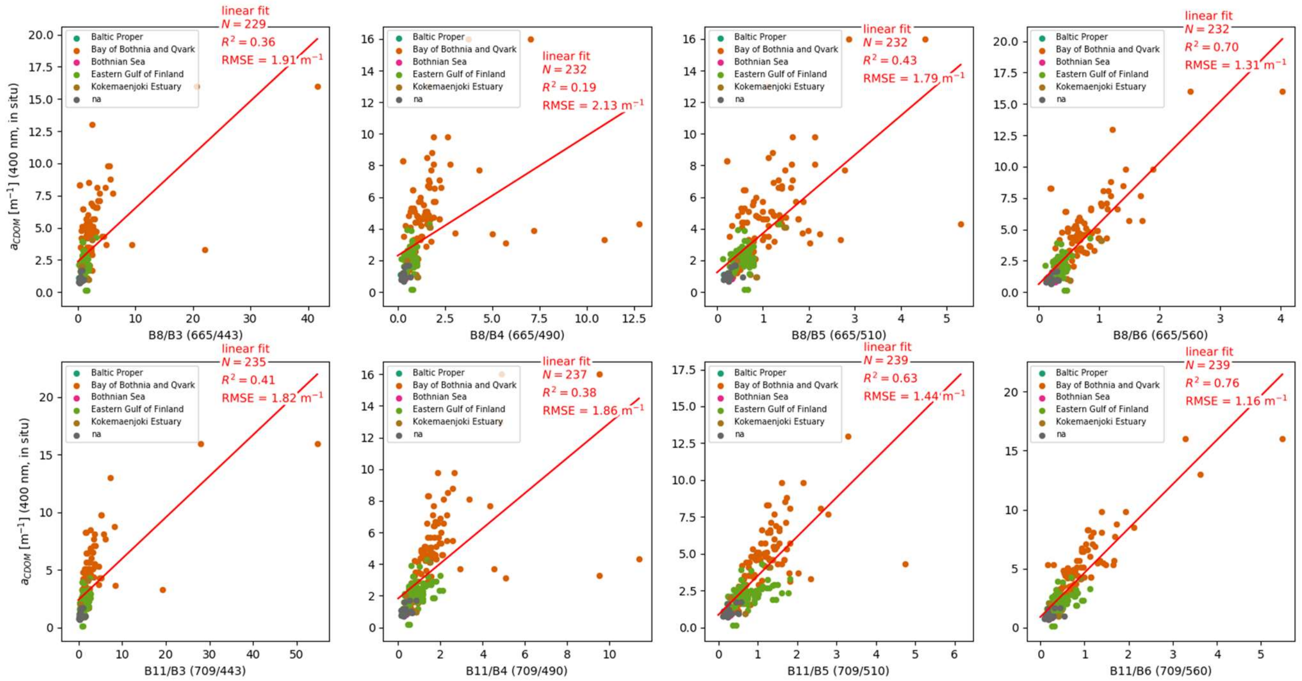

Figure 18. Sentinel-3 & Baltic+ reflectance band ratios vs. in situ aCDOM. Note that the wavelength used in the CDOM absorption coefficient is 400 nm.

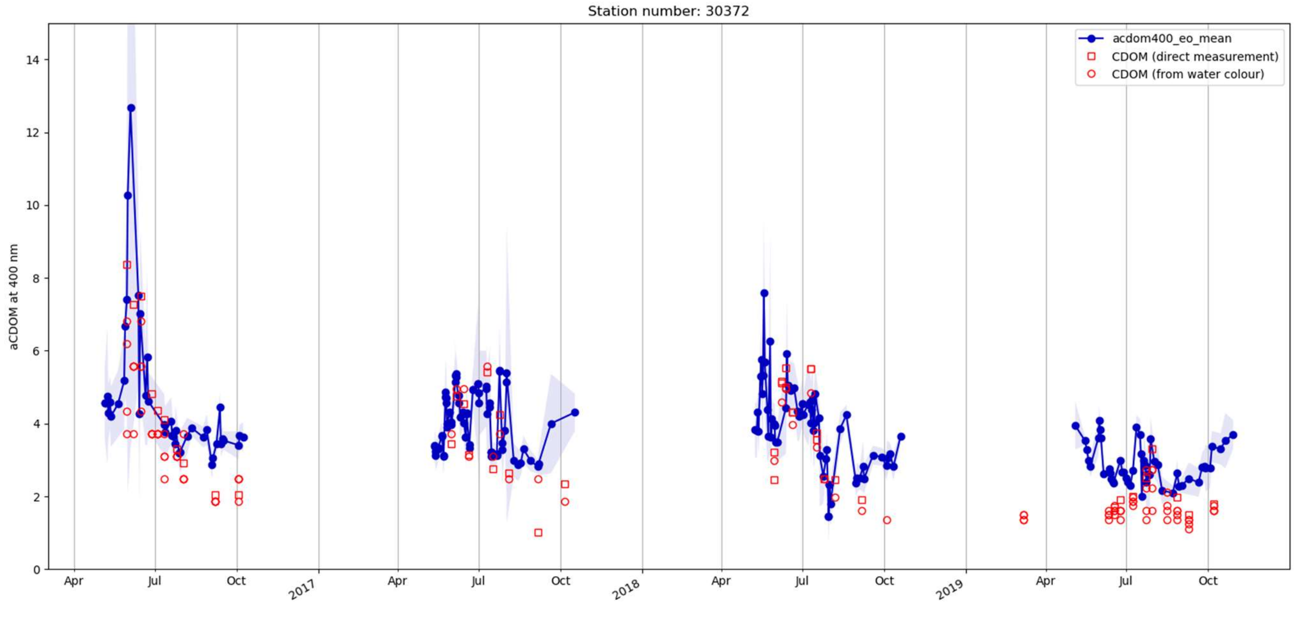

Figure 19. aCDOM timeseries measured in a laboratory from is situ samples and estimated from Sentinel-3 OLCI images with the band ratio rho_wn_8/rho_wn_6 (Eq. 1) at the Hailuoto intensive monitoring station.

3.4 Intercomparing Sentinel-2 MSI & c2rcc and Sentinel-3 OLCI & Baltic+ AC

Preparation for merging of Sentinel-2 and Sentinel-3 aCDOM products can include an intercalibration of these products. From satellite overpasses of the same days, several hundred macropixel were randomly selected from the Sentinel-2 aCDOM product. The macropixels have to consist entirely of valid pixels (using Idepix flag CLEAR_WATER, which states that there is a clear atmosphere above the water and excluding c2rcc CLOUD_RISK) and at the same time the ratio of standard deviation to mean value has to be below 15%. Noisy patches of the aCDOM map, which can be caused by submerged ice, where the atmospheric correction is bound to fail, are excluded in that way. The center pixel position of the homogenous macropixel becomes the extraction point for a single pixel of the Sentinel-3 product, given that it is valid (using Idepix flags not land, not snow/ice, not cloud or cloud buffer).

The aCDOM products are thus the mean value of the macropixel from S2-MSI (resampled to 60m) and the single full resolution pixel (300m), so that they are supposed to cover the same area.

There are two aCDOM products of S2-MSI considered here: one is a band ratio algorithm using the atmospheric corrected water leaving reflectance after the application of c2rcc, the second one scales the c2rcc IOP product adg (combining gelbstoff and detritus absorption) to retrieve aCDOM.

$$a_{CDOM}(443nm) = 5.16\left(\frac{\rho_w(709)}{\rho_w(560)}\right)^{1.29} \tag{3.2}$$

$$a_{CDOM}(440nm) = 0.654\ iop_{adg}^{1.45} + 0.2 \tag{3.3}$$

These two S2-MSI aCDOM products (at 443nm and 440nm, Eq. (3.2) and (3.3)) are compared to the aCDOM of the OLCI band ratio algorithm, which has been calibrated for the Baltic+AC reflectances (Eq. (3.1), at 400nm).

In this example of 14th of May 2018, the homogeneous macropixel can be found closer to the coast and almost all within one camera of Sentinel-2B. The aCDOM products based on band ratio algorithms (Figure 20, left, orange crosses) behave in a very clear linear fashion over the entire range of values to one another, which would allow an easy transformation of the one product into the other. The adg based aCDOM (blue crosses) show a S-shape in relation to the S3-OLCI band ratio. This behavior can be traced back to the underlying neural networks, which might show such nonlinear features close to the upper and lower limits of their training range.

Other examples (not shown here) suggest that for a full characterization of the necessary transformations the correlations would have to be studied as functions of the cameras which are involved.

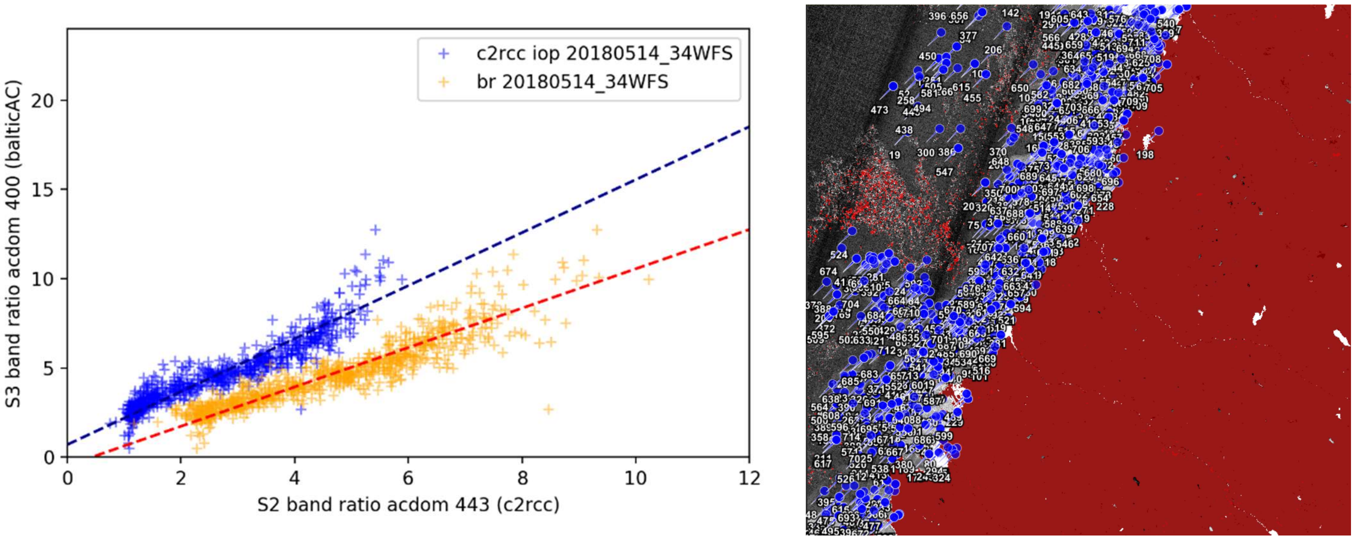

Figure 20. Selection of valid macropixels for S2B product (right, date 20180514, tile 34WFS, time difference to OLCI overpass 30min) falls into one camera near the coast. Band ratio algorithms of S2B C2RCC and S3A Baltic+AC show a well defined linear relationship (left, orange crosses). aCDOM derived from C2RCC adg (blue crosses) show a S-shape in relation to the S3-OLCI band ratio.

4 Validation summary

Based on these results the new Baltic+ processor provides the best atmospherically corrected reflectances when compared to other currently available processors (C2RCC, IPF). The estimation accuracy of aCDOM (with a band ratio algorithm) also improves when compared to earlier processors. The estimation accuracy with OCLI is now better than with S2 and C2RCC.

References

Antoine, D. and A. Morel (1999). A multiple scattering algorithm for atmospheric correction of remotely-sensed ocean colour (MERIS instrument): principle and implementation for atmospheres carrying various aerosols including absorbing ones, IJRS, 20, 1875-1916.

Bailey, S.W., and P. J. Werdell (2006). A multi-sensor approach for the on- orbit validation of ocean color satellite data products. Remote Sens. Environ. 102(1-2), 12–23.

Brockmann, C., Doerffer, R., Peters, M., Stelzer, K., Embacher, S., Ruescas, A. (2016). Evolution of the C2RCC neural network for Sentinel 2 and 3 for the retrieval of ocean colour products in normal and extreme optically complex waters. European Space Agency, (Special Publication) ESA SP, SP-740

EUMETSAT (2019). Recommendations for Sentinel-3 OLCI Ocean Colour product validations in comparison with in situ measurements – Matchup Protocols. http://www.eumetsat.int/website/wcm/idc/idcplg?IdcService=GET_FILE&dDocName=PDF_S3_OLCI_MATCHUP_PROTOCOLS_RECC&RevisionSelectionMethod=LatestReleased&Rendition=Web

K. Kallio, Sampsa Koponen, Jenni Attila, Mikko Kervinen, Timo Pyhälahti, Carsten Brockmann, Tonio Fincke, Lena Kritten (2014). Sentinel-2 MSI in the Monitoring of Lakes and Coastal Waters in Finland: Spectral and Spatial Resolution Considerations. Sentinel-2 for Science Workshop, ESRIN, May 20-22 2014. http://seom.esa.int/S2forScience2014/files/02_S2forScience-WaterII_KALLIO.pdf

Steinmetz, F., Deschamps, P.-Y., and Ramon, D. (2011). Atmospheric correction in presence of sun glint: application to MERIS. Optics Express, Vol. 19, Issue 10: 9783-9800.

Zibordi, G., B. Holben, I. Slutsker, D. Giles, D. D'Alimonte, F. Mélin, J.F. Berthon, D. Vandemark, H. Feng, G. Schuster, B.E. Fabbri, S. Kaitala, and J. Seppälä (2009): AERONET-OC: A Network for the Validation of Ocean Color Primary Products. J. Atmos. Oceanic Technol., 26, 1634–1651,